

# Synthesis and Characterization of Mono-, Di-, and Tri-Poly(ethylene glycol) Chlorin $e_6$ Conjugates for the Photokilling of Human Ovarian Cancer Cells

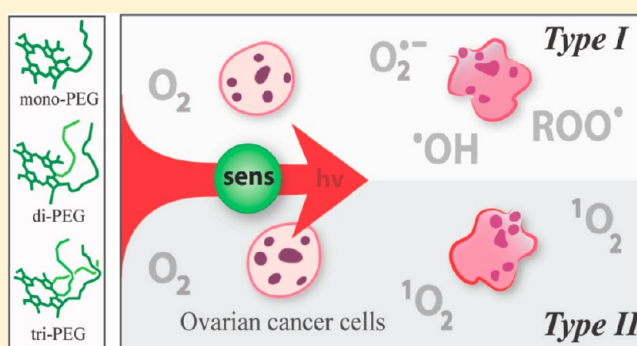
Stanley Kimani,<sup>†,‡</sup> Goutam Ghosh,<sup>†</sup> Ashwini Ghogare,<sup>†</sup> Benjamin Rudshiteyn,<sup>†</sup> Dorota Bartusik,<sup>†</sup> Tayyaba Hasan,<sup>\*,‡</sup> and Alexander Greer<sup>\*,†</sup>

<sup>†</sup>Department of Chemistry and Graduate Center, City University of New York, Brooklyn College, Brooklyn, New York 11210, United States

<sup>‡</sup>Wellman Center for Photomedicine, Massachusetts General Hospital and Harvard Medical School, Boston, Massachusetts 02114, United States

## S Supporting Information

**ABSTRACT:** PEGylated chlorin  $e_6$  photosensitizers were synthesized with tri(ethylene glycol) attached at the ester bond(s) for a 1:1 conjugate at the 17<sup>3</sup>-position, a 2:1 conjugate at the 15<sup>2</sup>- and 17<sup>3</sup>-positions, and a 3:1 conjugate at the 13<sup>1</sup>-, 15<sup>2</sup>-, and 17<sup>3</sup>-positions. These chlorin sensitizers were studied for hydrolytic stability and solubility, as well as ovarian OVCAR-5 cancer cell uptake, localization, and phototoxicity. Increasing numbers of the PEG groups in the mono-, di-, and tri-PEG chlorin conjugates increased the water solubility and sensitivity to hydrolysis and uptake into the ovarian cancer cells. The PEG chlorin conjugates accumulated in the cytoplasm and mitochondria, but not in lysosomes. Higher phototoxicity was roughly correlated with higher numbers of PEG groups, with the tri-PEG chlorin conjugate showing the best overall ovarian cancer cell photokilling of the series. Singlet oxygen lifetimes, solvent deuteration, and the effects of additives azide ion and D-mannitol were examined to help clarify the photokilling mechanisms. A Type-II (singlet oxygen) photosensitized mechanism is suggested for the di- and tri-PEG chlorin conjugates; however, a more complicated process based in part on a Type-I (radicals or radical ions) mechanism is suggested for the parent chlorin  $e_6$  and the mono-PEG chlorin conjugate.



## INTRODUCTION

A number of contributions have been made to understanding chlorin sensitizers in photodynamic therapy<sup>1</sup> and ovarian cancer killing reactions,<sup>2</sup> where substitution on the chlorin is done to overcome poor sensitization efficiency from aggregate formation<sup>3</sup> and low aqueous solubility. A PEGylated polymer (PEG 8000) chlorin  $e_6$  was studied, where the large PEG served as a solubilizing agent, inverting philicity from hydrophobic to hydrophilic.<sup>2</sup> Chlorin  $e_6$  has been covalently attached to bovine serum albumin (BSA) for selective photokilling of J774 murine macrophage-like cells instead of ovarian OVCAR-5 cancer cells.<sup>4</sup> Subcellular localization has been observed in *N*-(2-hydroxypropyl) methacrylamide copolymer chlorin  $e_6$  mono-ethylenediamine conjugates in a human ovarian carcinoma.<sup>5</sup>

Our hypothesis was that the PEG substituent numbers are adjustable for the photokilling activity of ovarian cancer cells in relation to each other. Thus, we have prepared PEG conjugated chlorin  $e_6$  photosensitizers, where one (1), two (2), and three (3) of the carboxylic acid groups were modified by a short 160 amu tri(ethylene glycol) chain [CH<sub>3</sub>(OCH<sub>2</sub>CH<sub>2</sub>)<sub>3</sub>OH] (Figure 1). The aims of the present work were to determine the

chemistry: (1) whether chlorins could be synthesized with increased numbers of attached PEG groups from 0 to 3, (2) whether the PEG-chlorin ester groups were highly labile to hydrolysis, (3) the extent to which the PEG groups enhanced solubility, (4) the computed conformations of the PEG groups via molecular mechanics and density functional theory calculations; and the photobiology: (5) the degree to which the PEGylated chlorins were taken up and localized into ovarian OVCAR-5 cancer cells, (6) whether the number of attached PEG groups influenced chlorin phototoxicity, and (7) mechanistic considerations of the phototoxicity based on H<sub>2</sub>O vs D<sub>2</sub>O solvent effects, singlet oxygen ( $\tau_{\Delta}$ ) lifetimes, and azide ion and D-mannitol additives. The results obtained here point to 3 as a potent ovarian cancer phototherapeutic agent.

## RESULTS AND DISCUSSION

**Synthesis and Characterization.** The addition of the [CH<sub>3</sub>(OCH<sub>2</sub>CH<sub>2</sub>)<sub>3</sub>OH] PEG to chlorin  $e_6$  relied on an *N*-(3-

Received: August 31, 2012

Published: November 5, 2012

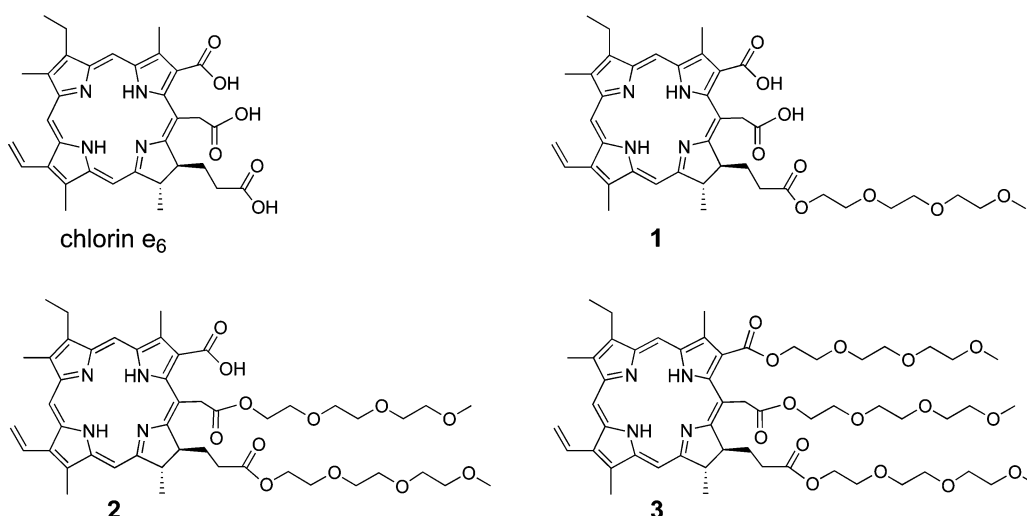


Figure 1. Parent chlorin *e*<sub>6</sub> and PEGylated chlorins 1–3.

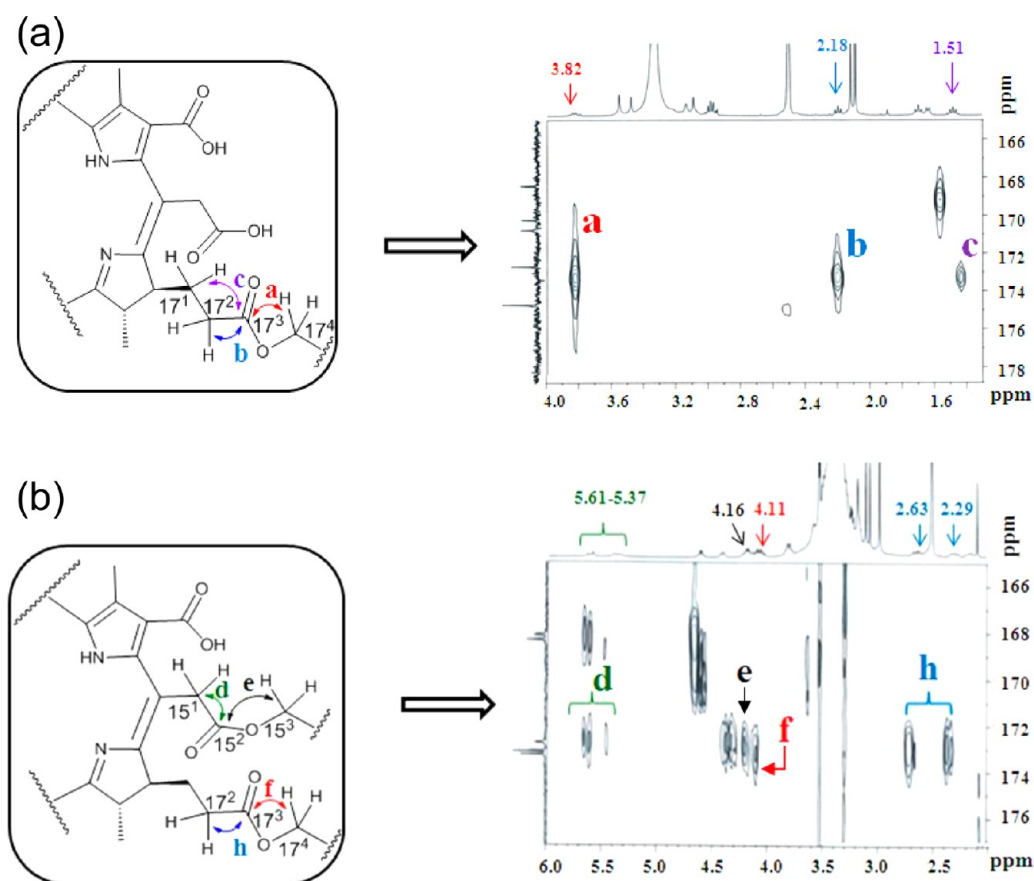


Figure 2. (a) The expanded 2D HMBC spectrum of **1** in DMSO-*d*<sub>6</sub> shows three sets of signals detected for the 17<sup>3</sup> carbonyl carbon coupled to protons attached to the 17<sup>1</sup>, 17<sup>2</sup>, and 17<sup>4</sup> carbons. Red “a” suggests  ${}^3J_{\text{C,H}}$  (17<sup>3</sup>, 17<sup>4</sup>), and 17<sup>4</sup> carbons. Red “a” suggests  ${}^3J_{\text{C,H}}$  (17<sup>3</sup>, 17<sup>4</sup>), and purple “c” suggests  ${}^3J_{\text{C,H}}$  (17<sup>3</sup>, 17<sup>1</sup>) coupling. (b) The expanded 2D HMBC spectrum of **2** in DMSO-*d*<sub>6</sub> shows four sets of signals for the 17<sup>3</sup> and 15<sup>3</sup> carbonyl carbon coupled to protons attached to the 17<sup>4</sup>, 17<sup>2</sup> and 15<sup>3</sup>, 15<sup>1</sup> carbons, respectively. Red “f” suggests  ${}^3J_{\text{C,H}}$  (17<sup>3</sup>, 17<sup>4</sup>), blue “h” suggests  ${}^2J_{\text{C,H}}$  (17<sup>3</sup>, 17<sup>2</sup>) coupling, black “e” suggests  ${}^3J_{\text{C,H}}$  (15<sup>2</sup>, 15<sup>3</sup>), and green “d” suggests  ${}^2J_{\text{C,H}}$  (15<sup>2</sup>, 15<sup>1</sup>) coupling.

dimethylaminopropyl)-*N'*-ethylcarbodiimide hydrochloride (EDC) condensation reaction in the formation of ester groups. Chlorin *e*<sub>6</sub> reacted with EDC, *N,N*-dimethyl-4-aminopyridine (DMAP), and CH<sub>3</sub>(OCH<sub>2</sub>CH<sub>2</sub>)<sub>3</sub>OH to produce **1** in 50% and **2** in 48% overall yields in 24 h, while 48 h periods produced **3** in 33% overall yield. According to HPLC, the purity of **1** was 94.7%, of **2** was 99.2%, and of **3** was 99.9%. Higher solubility

chlorins were easier to purify, as has been noted by others as well.<sup>6</sup> LC–MS data indicated that **1** contained one PEG group (MS calcd for C<sub>41</sub>H<sub>51</sub>N<sub>4</sub>O<sub>9</sub> [M + H]<sup>+</sup> = 743.3651, found 743.3673), **2** contained two PEG groups (MS calcd for C<sub>48</sub>H<sub>65</sub>N<sub>4</sub>O<sub>12</sub> [M + H]<sup>+</sup> = 889.4593, found 889.4586), and **3** contained three PEG groups (MS calcd for C<sub>55</sub>H<sub>79</sub>N<sub>4</sub>O<sub>15</sub> [M +

$H]^+ = 1035.5536$ , found 1035.5538). LC–MS provided mass identification for 1–3 but gave no information about structure.

1D  $^{13}C$  and 2D NMR experiments enabled the regiochemical assignments of the PEGs for the chlorin carboxy sites. For 1 and 2, the  $^{13}C$  NMR spectra indicated 20  $sp^2$  chlorin core carbons and 3 carbonyl carbons for total 23 signals within 93.5–174.7 ppm. The 23 carbon signals for each indicate that 1 and 2 formed as single isomers and not as a mixture of isomers. Mono-, di-, and tri-PEG attachments to 1, 2, and 3, respectively, was also evident due to the observation of 7, 14, and 21  $^{13}C$  NMR signals, respectively, coming in the region of 58–73 ppm. Figure 2 is the expanded portion of HMBC spectra for 1 and 2. For 1, a portion of the HMBC spectrum is shown in Figure 2A where three sets of signals detected for the  $17^3$  (172.7 ppm) carbonyl carbon coupled to protons attached to the  $17^1$  (1.51 ppm),  $17^2$  (2.18 ppm), and  $17^4$  (3.82 ppm) carbons, suggesting a linkage between the  $17^3$  carbonyl carbon and the PEG. In accord with a previous study,  $^1H$  NMR assigned protons of chlorin  $e_6$  trimethyl ester attached to  $17^1$  and  $17^2$  carbons at 1.75 and 2.19 ppm, respectively, as a multiplet<sup>7</sup> assisted us in assigning the  $17^1$  and  $17^2$  carbons of 1. Earlier work<sup>8</sup> with a monoamide chlorin  $e_6$  conjugate had shown the  $\delta$  values for 1.7 and 2.4 ppm for the protons connected to  $17^1$  and  $17^2$  carbons, respectively. Thus, we assigned the PEG to be attached at the  $17^3$  site in 1. In 1, other regioisomers were ruled out by analyzing the coupling between  $17^3$  carbonyl carbon and protons attached to the  $17^1$ ,  $17^2$ , and  $17^4$  carbons. Correlations between  $15^2$  carbonyl carbon and protons attached to  $15^1$  chlorin  $e_6$  core carbon and  $15^3$  PEG carbon were not found, and a correlation between PEG hydrogens and  $13^1$  carbonyl carbon was also not found. For 2, the HMBC spectrum in Figure 2B showed two sets of signals for the  $15^2$  (173.1 ppm) carbonyl carbon coupled to the protons attached to the  $15^1$  (5.37–5.61 ppm) and  $15^3$  (4.16 ppm) PEG carbons. Another two sets of signals for the  $17^3$  (173.3 ppm) carbonyl carbon to the protons attached to  $17^2$  (2.29 and 2.63 ppm) carbon and  $17^4$  (4.11 ppm) PEG carbon suggesting a linkage between the  $15^2$  and  $17^3$  carbonyl carbons and two PEGs in 2. In 2, other regioisomers were ruled out by analyzing the coupling between  $15^2$  carbonyl carbon and protons attached to the  $15^1$  and  $15^3$  carbons. A correlation between PEG hydrogens and the  $13^1$  carbonyl carbon was not observed. For 3, evidence for the attachment of three PEGs to all vacant chlorin  $e_6$  acid sites was provided by HSQC experiments. Twenty-one PEG carbons signals were observed (7 from each PEG) bearing protons that appeared as multiplets ranging from 3.29 to 4.08 ppm.

**Hydrolytic Stability.** The hydrolytic stability of the PEGylated chlorins 1–3 was measured with the solvent conditions [ $CH_3OH/H_2O$  (9:1)] matched to LC–MS eluent conditions, with the pH adjusted to 2.0 or 8.0 by formic acid or ammonium hydroxide (Table 1). The PEG groups attached to chlorin  $e_6$  did not spontaneously hydrolyze, although the solvolysis rates were increased as the number of PEG groups increased. After 4 h at pH 2.0, the solvolysis of 1 was 28%, of 2 was 57%, and of 3 was 100%. After 4 h at pH 8.0, the solvolysis of 1 was 21%, of 2 was 29%, and of 3 was 100%. Acid or alkaline methanol/water treatment of chlorin 3 led to the formation of 1, 2, and native chlorin  $e_6$ . Clearly, the hydrolysis rate was increased for 3 compared to that of 2 and 1, but the rates of sequential loss of each PEG were not scrutinized. Also, we have not examined the relative lability of the  $13^1$ ,  $15^2$ ,  $17^3$  ester bonds upon incorporation of chlorins 1–3 into the

**Table 1. Stability of PEGylated Chlorins 1–3**

pH	time	% disappearance of compound <sup>a</sup>		
		1	2	3
2.0	5 min	17	23	25
	1 h	17	39	81
	4 h	28	57	100
8.0	5 min	2	3	7
	1 h	18	18	100
	4 h	21	29	100

<sup>a</sup>LC–MS was used to follow the reaction (retention time  $t_R$  for 1, 2, and 3 was 7.10, 8.09, and 12.20 min, respectively). Values are an average of 3 or 4 measurements.

OVCAR-5 cells (described in Cellular Uptake and Subcellular Localization), although cancer cells are slightly acidic compared to normal cells, which would increase PEG ester lability.<sup>9,10</sup> There are reports of esterases dePEGylating vesicles, liposomes, and proteins modified with ester groups in ~2–10 h where the length and number of PEG chains and micellar properties modulate the esterase activity,<sup>11,12</sup> although ester bonds in prodrugs can persist in cells for longer periods.<sup>13</sup> Unlike the drug conjugates PEG/camptothecin<sup>14</sup> and PEG/gentamicin,<sup>15</sup> release of chlorin  $e_6$  from the PEG substituents was not a prerequisite for biological activity.

**Intrinsic Solubilities.** Table 2 lists the intrinsic solubilities of chlorin  $e_6$  and 1–3 that were measured in 1 % (v/v) DMSO

**Table 2. Effect of Increasing the Number of PEG Groups on Chlorin  $e_6$  on the Solubility and Computed Octanol/Water Partition Coefficients**

compound	number of PEG groups	solubility in 1 % (v/v) DMSO water <sup>a</sup> (mol/mL)	C log $P$ <sup>b</sup>
chlorin $e_6$	0	$1.8 \pm 1.3$	$6.59 \pm 1.74$
1	1	$2.3 \pm 1.0$	$5.61 \pm 1.65$
2	2	$3.3 \pm 0.9$	$5.56 \pm 1.67$
3	3	$3.9 \pm 0.8$	$4.70 \pm 1.68$

<sup>a</sup>Measurements were conducted three times, and the solubility value was averaged. <sup>b</sup>The C log  $P$  values were calculated with the ACD program.<sup>18</sup>

water (a solvent system that is practical and seemed biologically relevant, although the OVCAR-5 cell work in Cellular Uptake and Subcellular Localization uses only ~0.02 % (v/v) DMSO). Aliquots of 1% DMSO water were added to 50  $\mu g$  quantities of chlorin  $e_6$  or 1–3 with stirring for 1 h at room temperature and then allowed to stand for 5 h. Solution was filtered to separate insoluble compounds, and the amount of compound in the filtrate was determined by monitoring the Soret bands of chlorin  $e_6$  and 1–3. The mono- (1), di- (2), and tri-PEG (3) chlorin conjugates were increasingly soluble. By comparison to the parent chlorin  $e_6$ , chlorins 1–3 had an enhanced solubility of 1.6–3.6-fold. Similar factors that make the PEGylated chlorins more soluble in 1 % (v/v) DMSO water affected their octanol/water partition coefficients. Computed log  $P$  values were obtained with the ACD algorithm, which has performed well in predicting the log  $P$  values of drugs,<sup>16</sup> and PEG groups introduce steric hindrance to the sites in which they are bound.<sup>17</sup> We find C log  $P$  values to decrease by about 2 orders of magnitude as the number of attached PEG groups increased from 0 to 3.

**Computed Conformations.** Aggregation can reduce photosensitization efficiency, such as the reduced excited-state lifetimes of aggregated glycoconjugated sensitizers.<sup>19</sup> Increased numbers of PEGs in 1–3 leading to increasingly hindered porphyrins would be expected to reduce self-aggregation, especially when compared to the parent unsubstituted chlorin  $e_6$  compound. Monte Carlo calculations were carried out on 1–3 with the MM+ force field (Figure 3). In each case, the 10

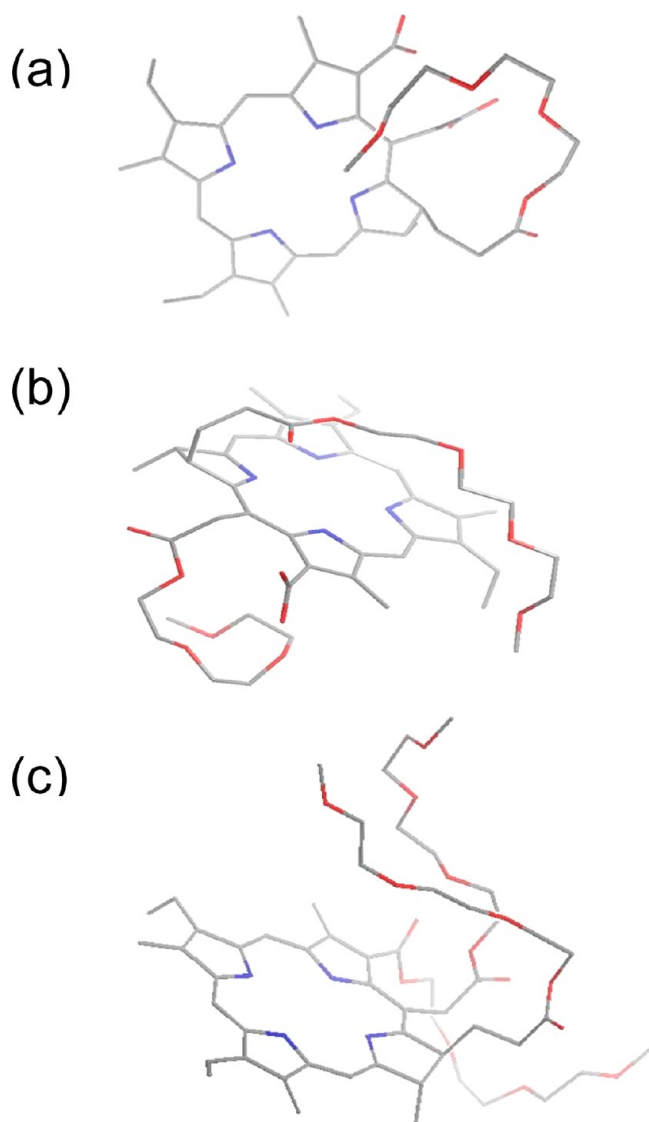


**Figure 3.** Examples of three low-energy minima computed by molecular mechanics (MM+) and B3LYP/6-31G(d) methods. (a) A structure optimized with the PEG curled above the chlorin ring in 1, (b) a structure with two PEGs, one curled above and the other below the chlorin ring in 2, and (c) a structure with two of the three PEGs curled above the chlorin ring in 3.

lowest energy MM+ conformations<sup>20</sup> were taken and reoptimized with B3LYP/6-31G(d)<sup>21</sup> in the gas phase. Low energy B3LYP conformations showed some curling of the PEG groups onto the porphyrin ring. In a rather cursory study, we found many curled PEG conformers to be slightly lower in energy than uncurled conformers. Figure 3 shows an instance where two PEG groups were distributed over both faces of the porphyrin in 2. Li et al.<sup>22</sup> observed curling of an attached PEG onto a hematoporphyrin ring using solution-phase molecular

dynamics simulations, and “curling” of long fatty acid chains is directly related to dynamics in phospholipid membranes.<sup>23</sup> Carried to a greater extreme than PEGylation, cyclodextrins have been used to encapsulate photosensitizers to better ensure maintenance of a monomeric state.<sup>24,25</sup>

**Cellular Uptake and Subcellular Localization.** We examined the uptake of chlorin  $e_6$  and 1–3 in ovarian OVCAR-5 cancer cells after 4 h of incubation in complete Roswell Park Memorial Institute (RPMI) 1640 media. Figure 4

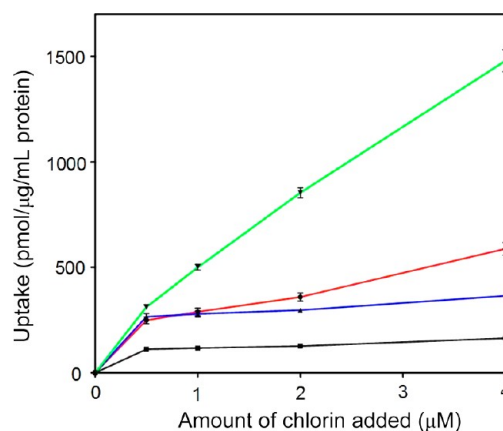


**Figure 4.** Uptake of chlorin  $e_6$  (black line), 1 (blue line), 2 (red line), and 3 (green line) by OVCAR-5 cells as a function of concentration. The cells were incubated with 0.5, 1.0, 2.0, and 4.0  $\mu\text{M}$  concentrations of the chlorins in media for 4 h. Cells were then lysed in 0.1 M NaOH/1% sodium dodecyl sulfate (SDS) for 24 h, and the concentrations of the chlorins were determined by fluorescence measurements. Each point represents the mean of three independent experiments (mean  $\pm$  SEM), each one performed in triplicate.

shows that the cellular uptake was higher for PEGylated 1–3 compared to the parent “unsubstituted” chlorin  $e_6$  over the concentration range tested, 0.5–4.0  $\mu\text{M}$ . An increased number of PEG groups in chlorins 1–3 tended to increase the cellular uptake. The cellular uptake of 3 was 1.2–6.0-fold better than that of 1. The uptake of 3 had not plateaued at the highest concentration tested (4.0  $\mu\text{M}$ ), and the time-dependence of the cellular uptake was not investigated.

Subcellular localization of the chlorins was also studied. Chlorin  $e_6$  or 1–3 (1.0  $\mu\text{M}$ ) were added to the OVCAR-5 cells. The samples were then incubated for 4 h with either 50 nM mitotracker green or 50 nM lysotracker. Figure 5 and Figures S22 and S23 (Supporting Information) show that the chlorin  $e_6$  or 1–3 photosensitizers (red fluorescence) were spread throughout the cytoplasm and in the mitochondria based on co-localization with the mitotracker probe (green fluorescence). No evidence was found for co-localization of the chlorin photosensitizers in lysosomes using the lysotracker probe (green fluorescence), nor were there differences in subcellular localization of the chlorins as evidenced by yellow color in the confocal images. Differences in subcellular localization have been seen in glucoconjugated chlorins<sup>26</sup> and in mono-L-aspartyl chlorin  $e_6$ .<sup>27,28</sup>

**Photodynamic Killing of Ovarian Cancer Cells.** Figure 6 shows sensitized phototoxicity effects of chlorin  $e_6$  and 1–3 to OVCAR-5 cell viabilities analyzed 24 h postirradiation using a 3-(4,5-dimethylthiazol-2-yl)-2,5-diphenyltetrazolium bromide (MTT) assay. In these studies, OVCAR-5 cells were incubated for 4 h with 0.01, 0.1, and 1.0  $\mu\text{M}$  chlorin  $e_6$  or 1–3 prior to

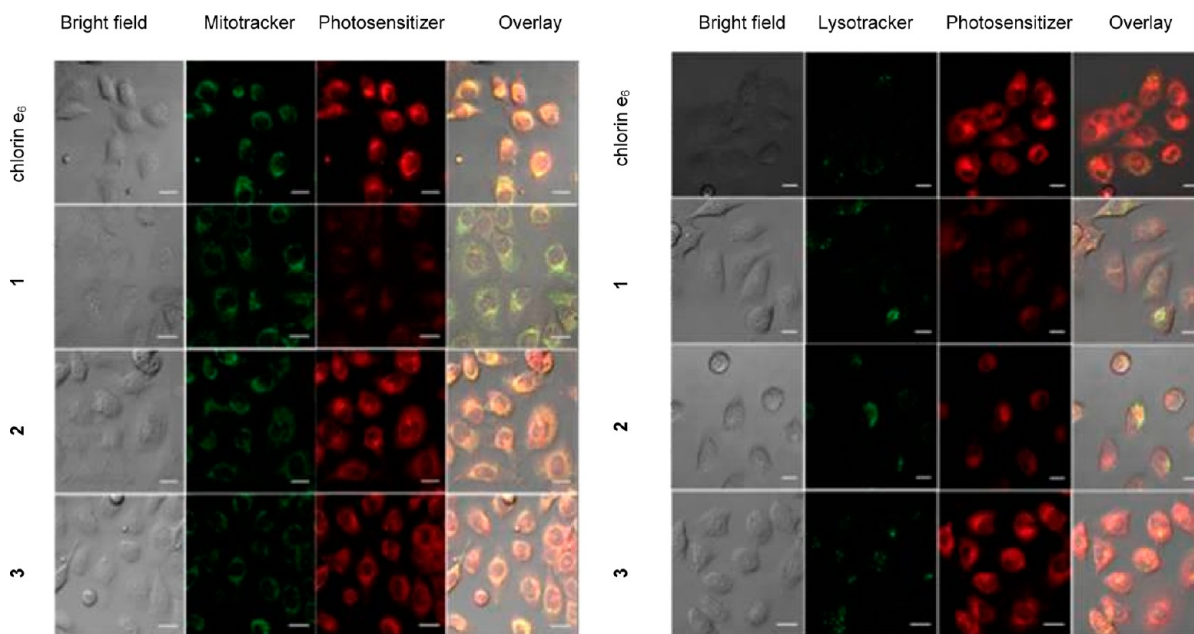


**Figure 5.** Subcellular localization of chlorin  $e_6$  and 1–3 in OVCAR-5 cells using fluorescence microscopy. The cells were incubated with 1.0  $\mu\text{M}$  chlorin  $e_6$  or 1–3 for 4 h (red fluorescence). In the final 30 min of the incubation, the cells were counterstained with 50 nM mitotracker green or lysotracker (green fluorescence). Magnification 100 $\times$ ; bar scale = 50  $\mu\text{m}$ .

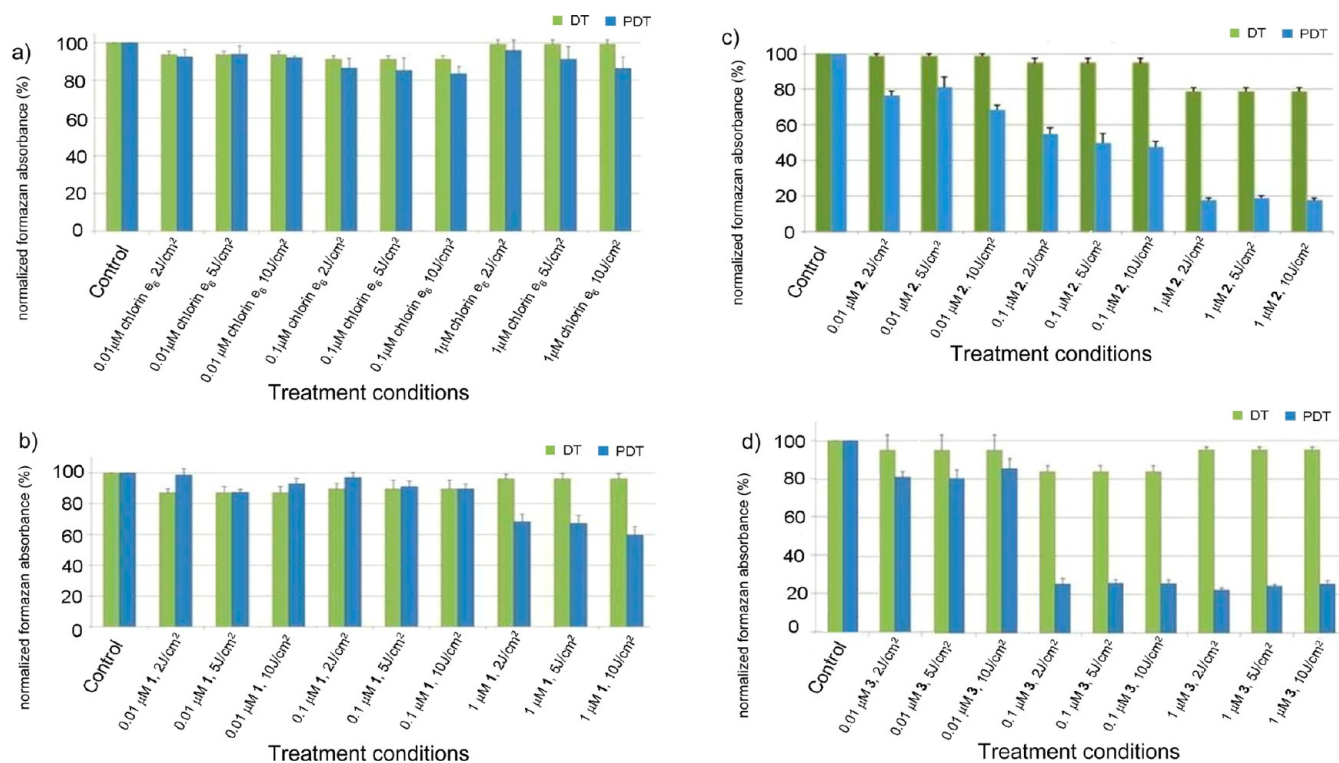


**Figure 6.** Phototoxicity effects on OVCAR-5 cells treated with 0.01, 0.1, and 1.0  $\mu\text{M}$  chlorin  $e_6$  (plot a), 1 (plot b), 2 (plot c), or 3 (plot d), irradiated with 670 nm laser at 2, 5, or 10  $\text{J}/\text{cm}^2$  after 4 h of incubation. Cell viability was assessed by MTT assay, and results are shown as percent relative to control cells. Results represent the mean of three independent experiments for each condition (mean  $\pm$  SEM), performed in triplicate. DT = dark toxicity; PDT = phototoxicity.

irradiation with 670 nm laser light. Similar phototoxicity results were obtained with fluences ranging from 2 to 10  $\text{J}/\text{cm}^2$ . Dark toxicity was generally minimal, i.e. <10% in all cases, except 2 at 1.0  $\mu\text{M}$  and 3 at 0.1  $\mu\text{M}$ , which were  $\sim$ 20%. At 1.0  $\mu\text{M}$  concentrations, the PEGylated compounds 1–3 all showed higher phototoxicity compared to parent chlorin  $e_6$ . At 0.1  $\mu\text{M}$

concentrations, 2 and 3 were higher in phototoxicity when compared to both chlorin  $e_6$  and 1. The relationship between cellular uptake and photocytotoxicity of chlorin  $e_6$  or 1–3 was correlated, although not significantly. For example, at 1.0  $\mu\text{M}$  concentrations, uptake of 1 and 2 were identical but the phototoxicity of the latter was 50% greater. Another example, at

1.0  $\mu\text{M}$  concentrations is the 2-fold-enhanced uptake of **3** compared to **2**, where the same percent phototoxicity was observed. At present, attempts were not made to detect leakage from the cells after the photodynamic treatment.

**Mechanism of Phototoxicity.** Experiments were conducted to determine whether the phototoxicity mechanisms were dominated by Type-I (radicals or radical ions) or Type-II (singlet oxygen) photosensitized oxidation processes. Singlet oxygen lifetime ( $\tau_{\Delta}$ ) and phototoxicity data were collected in  $\text{H}_2\text{O}$ -based media (RPMI),  $\text{H}_2\text{O}$ -phosphate buffered saline (PBS), and  $\text{D}_2\text{O}$ -PBS with OVCAR-5 cells and chlorin  $e_6$  or **1–3** (0.1  $\mu\text{M}$ ). Studies were also carried out in the presence of sodium azide or D-mannitol.

With respect to changing the main solvent component from  $\text{H}_2\text{O}$  to  $\text{D}_2\text{O}$ , literature  $^1\text{O}_2$  ( $\tau_{\Delta}$ ) lifetimes show an increase of 20-fold.<sup>29–31</sup> Table 3 and Figure S24 (Supporting Information)

**Table 3. Lifetime of Singlet Oxygen ( $\tau_{\Delta}$ ) in  $\text{H}_2\text{O}$  and  $\text{D}_2\text{O}$  Solutions of Chlorin 2**

entry	medium	$\tau_{\Delta}^a$ ( $\mu\text{s}$ )
1	1 % (v/v) DMSO in $\text{D}_2\text{O}$	60
2	$\text{D}_2\text{O}$ -PBS containing 5 mM glucose, 1 % (v/v) DMSO, 90 % (v/v) $\text{D}_2\text{O}$ , 10 % (v/v) $\text{H}_2\text{O}$	52
3	1 % (v/v) DMSO in $\text{H}_2\text{O}$	3.2
4	PBS containing 5 mM D-glucose	2.9
5	RPMI media containing 10% FCS	2.7

<sup>a</sup>The  $^1\text{O}_2$  luminescence intensity was monitored. The monoexponential decay component of the  $^1\text{O}_2$  phosphorescence at 1270 nm was followed upon irradiation of **2** ( $5.2 \times 10^{-5}$  M) with 355 nm.

show the  $\tau_{\Delta}$  data in media containing  $\text{H}_2\text{O}$  and  $\text{D}_2\text{O}$ . In 1 % (v/v) DMSO  $\text{D}_2\text{O}$  solution, we have found the  $\tau_{\Delta}$  was 60  $\mu\text{s}$ , whereas in  $\text{D}_2\text{O}$ -PBS (cell-free) media, the  $\tau_{\Delta}$  was reduced to 52  $\mu\text{s}$ , which we mainly attribute to the 5-mM glucose and 10%  $\text{H}_2\text{O}$  contents of the latter. Our results are in-line with literature lifetime values of  $^1\text{O}_2$  in neat  $\text{H}_2\text{O}$  (3.3  $\mu\text{s}$ ).<sup>31</sup> Because  $\text{H}_2\text{O}$ -based RPMI media contains 10% fetal calf serum (FCS), where the cysteine, methionine, tryptophan, and histidine residues serve as  $^1\text{O}_2$  quenchers,<sup>32–34</sup>  $\tau_{\Delta}$  was reduced by  $\sim 0.6$   $\mu\text{s}$  compared to neat  $\text{H}_2\text{O}$ , which in part would explain the higher cell viability in irradiated samples in RPMI media compared to  $\text{H}_2\text{O}$ -PBS in Figure 7.

We find that phototoxicity increased with increasing number of PEGs, where **3** showed the highest phototoxicity (Figure 7). The dark toxicity was not affected significantly by changing the solvent from  $\text{D}_2\text{O}$  to  $\text{H}_2\text{O}$  in PBS. For **2** (but not chlorin  $e_6$ , **1**, and **3**), the results showed that the photokilling was increased in  $\text{D}_2\text{O}$ -PBS ( $P < 0.05$ ) compared to  $\text{H}_2\text{O}$ -RPMI. Studies were also carried out with sodium azide and D-mannitol in concentrations that were not toxic to the OVCAR-5 cells (Figure 8). Sodium azide (2 mM) decreased the phototoxicity of **2** by  $\sim 25\%$  ( $P < 0.001$ ) compared to **2** alone, and of **3** by 10% ( $P < 0.001$ ) compared to **3** alone. D-Mannitol (30 mM) decreased the phototoxicity of **2** by  $\sim 4\%$ , which was not statistically significant compared to **2** alone. With **3**, D-mannitol decreased the phototoxicity  $\sim 8\%$ , which was a statistically significant decrease ( $P < 0.01$ ) compared to **3** alone. The results with D-mannitol for chlorin  $e_6$  and **1** were reversed, that is, D-mannitol had little effect or promoted the phototoxicity.

We believe that PDT is often a mixture of Type I and II mechanisms. The data obtained here include intracellular and

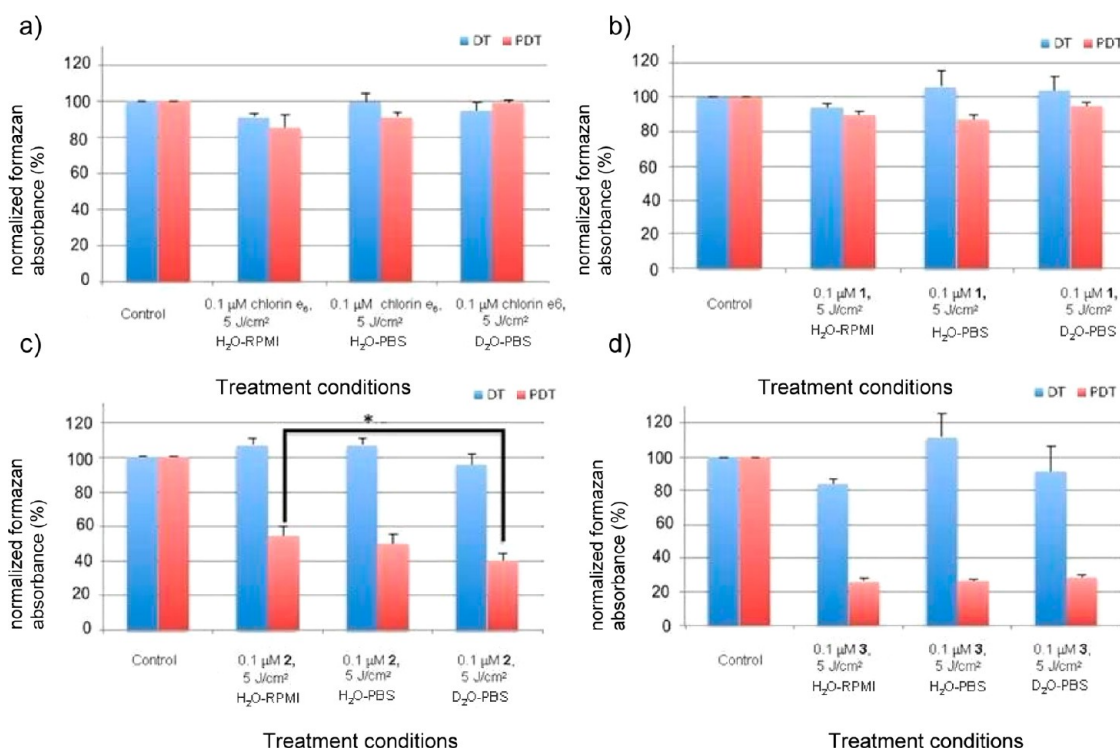


**Figure 7.**  $\text{H}_2\text{O}/\text{D}_2\text{O}$  solvent isotope effects on the phototoxicity of OVCAR-5 cells incubated with 0.1  $\mu\text{M}$  chlorin  $e_6$  (plot a), **1** (plot b), **2** (plot c), or **3** (plot d) for 4 h. The cells were then irradiated in  $\text{H}_2\text{O}$ -based media (RPMI),  $\text{H}_2\text{O}$ -based PBS, or  $\text{D}_2\text{O}$ -based PBS with 670 nm laser light (5 J/cm<sup>2</sup>) where phototoxicity was measured 24 h postirradiation. Results represent the mean of three independent experiments (mean  $\pm$  SEM) in triplicate. DT = dark toxicity; PDT = phototoxicity.

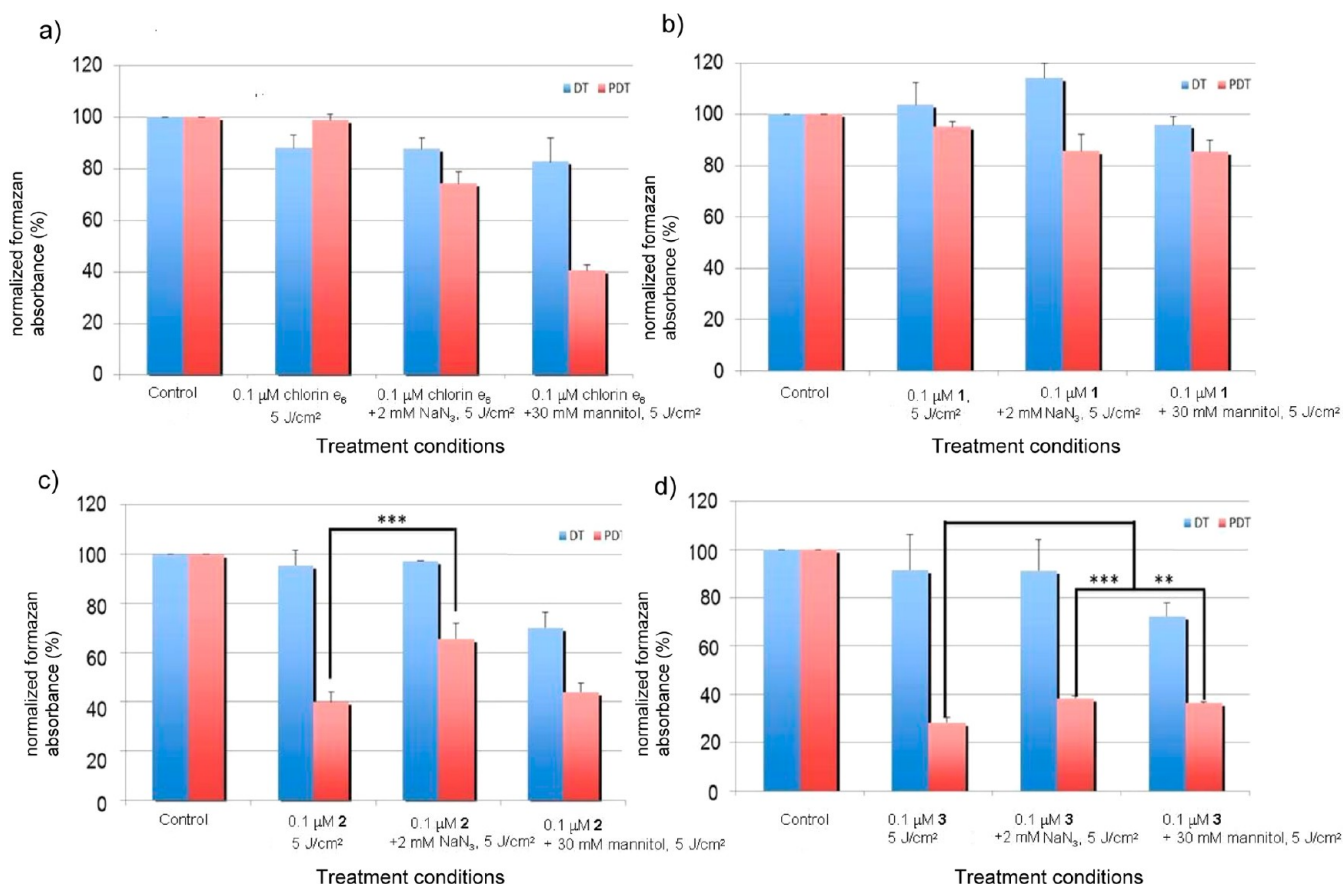


**Figure 8.** Effects of sodium azide and D-mannitol on the phototoxicity of chlorin  $e_6$  or 1–3 samples irradiated in  $\text{D}_2\text{O}$ -PBS. OVCAR-5 cells were incubated with 0.1  $\mu\text{M}$  chlorin  $e_6$  or 1–3 for 4 h. D-Mannitol (30 mM) or sodium azide (2 mM) was then added in the final 1 h of incubation. The cells were then irradiated in  $\text{D}_2\text{O}$ -based PBS with or without the D-mannitol or sodium azide, with 670 nm laser at a fluence of 5  $\text{J}/\text{cm}^2$ . After irradiation,  $\text{D}_2\text{O}$  was replaced with complete media, and the cells were further incubated for 24 h followed by analysis of the cell viability using MTT assay. Results represent the mean of at least two independent experiments (mean  $\pm$  SEM) in triplicate and analyzed by one-way ANOVA with Tukey's multiple comparison test. Statistically significant differences indicated by asterisks; \*\*\* $P < 0.001$ , \*\* $P < 0.01$ . DT = dark toxicity; PDT = phototoxicity.

extracellular effects and argue in favor of a Type-II mechanism for 2 and 3 and a more complicated process likely including a Type-I mechanism for chlorin  $e_6$  and 1. The lack of enhanced photokilling in  $\text{D}_2\text{O}$ -PBS for all chlorins tested was unexpected and may relate to factors such as longer triplet sensitizer lifetimes in  $\text{D}_2\text{O}$  compared to  $\text{H}_2\text{O}$ ,<sup>35,36</sup> with no associated effect on the population of free radicals, but also recognizing that oxygenated amino acids themselves can be toxic. Our cell samples were exposed to  $\text{D}_2\text{O}$  for only 30 min prior to photolysis and thus may have limited  $\text{D}_2\text{O}$  permeation into the mitochondria. Osmotic shock experiments were not conducted where  $\text{H}_2\text{O}$  will be more effectively replaced by  $\text{D}_2\text{O}$ , because the technique tends to stress OVCAR-5 cells. We are not invoking a mechanism of preferred penetration of  $\text{D}_2\text{O}$  over azide ion into the cells. It would be an exaggeration to claim singlet oxygen as the exclusive photokilling species under any condition here, or else the protective effect of azide ion would have been more remarkable. Even though the azide ion concentrations used (2 mM) were not expected to quench the triplet-excited state of the sensitizer in homogeneous solution,<sup>37</sup> in the cells there may be some contribution from this route due to localization effects with a further complication that azide ion can quench other molecular species including free radicals.<sup>38</sup>

## CONCLUSION

The following conclusions were drawn: (1) Short-chained PEGs were coupled to the carboxylic acid sites of chlorin  $e_6$ . The synthesis included a 1:1 conjugate 1 with chlorin  $e_6$  PEGylated at the 17<sup>3</sup>-position, a 2:1 conjugate 2 with chlorin  $e_6$  PEGylated at the 15<sup>2</sup>- and 17<sup>3</sup>-positions, and a 3:1 conjugate 3 with chlorin  $e_6$  PEGylated at the 13<sup>1</sup>-, 15<sup>2</sup>-, and 17<sup>3</sup>-positions. The regiochemistry of the addition of the PEG group(s) to chlorin  $e_6$  was based on 2D NMR and mass spectrometry data. (2) By the introduction of higher numbers of PEG groups, chlorins 1–3 were increasingly hydrolytically labile. (3) The mono- (1), di- (2), and tri-PEG (3) chlorin conjugates were increasingly soluble in aqueous DMSO solution. Computed log  $P$  values suggest successive lipophilic deamplification in chlorins 1–3 compared to chlorin  $e_6$ , by 1–2 log units. (4) Molecular mechanics and DFT calculations indicated that the PEGs can wrap onto the porphyrin face suggesting an increasing number of PEG groups will increasingly resist formation of aggregates held together by  $\pi$ - $\pi$  stacking forces. (5) With increasing numbers of PEG groups in 1–3, a steady increase in cellular uptake was observed in an in vitro model of human ovarian cancer. Accumulation of chlorin  $e_6$  and 1–3 was evident in the cytoplasm and mitochondria, but not in lysosomes. These chlorins did not show differential subcellular localization. (6) Increased numbers of PEG groups led to increased photo-

toxicity, where the increase roughly paralleled the cellular uptake. (7) For **2** and **3**, the data pointed to a Type-II mechanism based on azide ion quenching, whereas for chlorin  $e_6$  and **1** the situation is more complex where some contribution from a Type-I mechanism was evident. This brings us to our final point: because of our interest in fiber-based photosensitizer and singlet oxygen delivery methods,<sup>39</sup> desirable aspects of the tri-PEG chlorin conjugate, **3**, make it a potential sensitizer for incorporation into a fiber optic device, particularly for the area of ovarian cancer photodynamic therapy.

## EXPERIMENTAL SECTION

**General Information.** Methanol, dichloromethane, 1-octanol, chloroform- $d_1$ , deuterium oxide- $d_2$ , chlorin  $e_6$ , *N*-(3-dimethylamino-propyl)-*N'*-ethylcarbodiimide hydrochloride (EDC), *N,N*-dimethyl-4-aminopyridine (DMAP), and tri(ethylene glycol) monomethyl ether (TGEE, MW = 164.20) were used as received from commercial suppliers. Deionized water was purified using a deionization system. An HPLC chromatogram suggested the commercial chlorin  $e_6$  to be of 99.9% purity. Purification of the sensitizer mixtures was conducted by column chromatography using 200–400 mesh silica gel. TLC was carried out using silica gel 60F 254 TLC plates. Proton NMR data were acquired at 400 MHz, and <sup>13</sup>C NMR data were acquired at 100.6 MHz. UV-vis, HRMS, LC-MS, GC-MS, HPLC, steady-state fluorescence, and melting point data were collected. HPLC and LC-MS instruments were used as has been described in our previous work.<sup>40</sup> Light was delivered from either a 670 nm CW diode laser or a Minilase 10-Hz Nd:YAG Q-switched laser.

**Synthesis of 17<sup>3</sup>-Chlorin  $e_6$  Methoxy Tri(ethylene glycol) Ester (**1**).** Yield 0.056 g (50%); monomeric purity: 94.7%. Chlorin  $e_6$  (90.0 mg, 0.15 mmol) reacted with TGEE (178.20 mg, 1.10 mmol), EDC (28.0 mg, 0.15 mmol), and DMAP (18.3 mg, 0.15 mmol) in CH<sub>2</sub>Cl<sub>2</sub> (10.0 mL), which was stirred for 24 h under N<sub>2</sub> at room temperature. Purification of the residue was done by silica gel column eluting with 10% CH<sub>3</sub>OH in CHCl<sub>3</sub> yielding **1** as a sticky blue solid. *R*<sub>f</sub> = 0.10. <sup>1</sup>H NMR (400 MHz, DMSO- $d_6$ )  $\delta$  9.79 (s, 1H), 9.67 (s, 1H), 9.11 (s, 1H), 8.36 (dd, *J* = 17.6 Hz, 11.6 Hz, 1H), 6.45 (d, *J* = 18 Hz, 1H), 6.16 (d, *J* = 11.6 Hz, 1H), 6.00 (d, *J* = 19.6 Hz, 1H), 5.81 (d, *J* = 5.6 Hz, 2H), 5.45 (d, *J* = 11.6 Hz, 1H), 4.57 (d, *J* = 7.6 Hz, 2H), 4.35 (q, *J* = 8.8 Hz, 2H), 4.14 (m, 4H), 3.82 (m, 4H), 3.25 (m, 4H), 3.09 (s, 3H), 2.98 (m, 4H), 2.18 (m, 3H), 1.69 (m, 3H), 1.63 (d, *J* = 6.8 Hz, 2H), 1.51 (m, 3H), 1.48 (m, 1H), -1.97 (s, 1H), -2.5 (s, 1H). <sup>13</sup>C NMR (100.6 MHz, DMSO- $d_6$ )  $\delta$  174.7, 172.7, 170.7, 170.2, 168.4, 157.1, 153.7, 148.8, 144.9, 140.1, 138.6, 136.5, 135.3, 134.4, 134.3, 130.7, 129.7, 122.4, 107.3, 103.1, 101.6, 98.8, 94.6, 72.8, 72.7, 71.4, 70.2, 70.0, 69.8, 58.3, 53.1, 49.0, 38.1, 31.2, 30.0, 23.4, 19.3, 18.2, 12.5, 12.4, 11.4. HRMS (ESI) *m/z* calcd for [C<sub>41</sub>H<sub>50</sub>N<sub>4</sub>O<sub>9</sub> + Na]<sup>+</sup> 765.3470, found 765.3500. (ESI) *m/z* calcd for C<sub>41</sub>H<sub>51</sub>N<sub>4</sub>O<sub>9</sub> [M + H]<sup>+</sup> 743.3651, found 743.3673. UV-vis (CHCl<sub>3</sub>)  $\lambda_{\max}$  ( $\epsilon/M^{-1}cm^{-1}$ ) 665 nm (87868), 404 nm (272083).

**Synthesis of 17<sup>3</sup>,15<sup>2</sup>-Chlorin  $e_6$  Methoxy Tri(ethylene glycol) Diester (**2**).** Yield 0.035 g (48%); monomeric purity: 99.2%. Chlorin  $e_6$  (50.0 mg, 0.08 mmol) reacted with TGEE (32.0 mg, 0.4 mmol), EDC (30.0 mg, 0.16 mmol), and DMAP (19.5 mg, 0.16 mmol) in CH<sub>2</sub>Cl<sub>2</sub> (10.0 mL), which was stirred for 24 h under N<sub>2</sub> at room temperature. Purification of the residue was done by silica gel column eluting with 5% CH<sub>3</sub>OH in CH<sub>2</sub>Cl<sub>2</sub> yielding **2** as a sticky blue solid. *R*<sub>f</sub> = 0.21. <sup>1</sup>H NMR (400 MHz, DMSO- $d_6$ )  $\delta$  9.74 (s, 1H), 9.73 (s, 1H), 9.09 (s, 1H), 8.31 (dd, *J* = 17.6 Hz, 11.6 Hz, 1H), 6.65 (d, *J* = 6.8 Hz, 1H), 6.45 (d, *J* = 18 Hz, 1H), 5.61 (d, *J* = 19.0 Hz, 1H), 5.37 (d, *J* = 19.0 Hz, 1H), 4.61 (q, *J* = 7.2 Hz, 2H), 4.40 (m, 2H), 4.16 (m, 4H), 4.11 (m, 4H), 3.81 (m, 4H), 3.57 (m, 4H), 3.23 (s, 4H), 3.22 (s, 4H), 3.10 (s, 3H), 3.07 (s, 3H), 2.98 (s, 3H), 2.63 (m, 1H), 2.29 (m, 3H), 2.13 (m, 3H), 1.66 (t, *J* = 8.0 Hz, 3H), 1.64 (d, *J* = 8.0 Hz, 3H), -1.72 (s, 1H), -2.10 (s, 1H). <sup>13</sup>C NMR (100.6 MHz, DMSO- $d_6$ )  $\delta$  173.3, 173.1, 172.7, 168.3, 168.1, 152.2, 149.1, 144.0, 137.1, 136.5, 136.5, 133.4, 133.3, 133.0, 131.5, 130.0, 129.2, 121.7, 103.7, 99.8, 99.0, 94.3,

72.7, 71.5, 71.3, 70.0, 70.0, 69.9, 69.8, 69.8, 69.6, 68.7, 68.5, 64.2, 63.6, 60.7, 58.3, 53.3, 48.2, 37.9, 31.1, 29.9, 23.6, 19.4, 18.2, 12.5, 11.4. HRMS (ESI) *m/z* calcd for [C<sub>48</sub>H<sub>64</sub>N<sub>4</sub>O<sub>12</sub> + Na]<sup>+</sup> 911.441, found 911.432. (ESI) *m/z* calcd for C<sub>48</sub>H<sub>65</sub>N<sub>4</sub>O<sub>12</sub> [M + H]<sup>+</sup> 889.4593, found 889.4586. UV-vis (CHCl<sub>3</sub>)  $\lambda_{\max}$  ( $\epsilon/M^{-1}cm^{-1}$ ) 664 nm (94342), 404 nm (285333).

**Synthesis of 17<sup>3</sup>,15<sup>2</sup>,13<sup>1</sup>-Chlorin  $e_6$  Methoxy Tri(ethylene glycol) Triester (**3**).** Yield 0.014 g (33.0%); monomeric purity: 99.9%. Chlorin **2** (36.0 mg, 0.04 mmol) reacted with TGEE (0.50 g, 3.04 mmol), EDC (23.04 mg, 0.12 mmol), and DMAP (14.64 mg, 0.12 mmol) in CH<sub>2</sub>Cl<sub>2</sub> (10.0 mL), which was stirred for 24 h under N<sub>2</sub> at room temperature. Purification of the residue was done by silica gel column eluting with 1% CH<sub>3</sub>OH in CH<sub>2</sub>Cl<sub>2</sub> yielding **3** as a sticky blue solid. *R*<sub>f</sub> = 0.5. <sup>1</sup>H NMR (400 MHz, DMSO- $d_6$ )  $\delta$  9.76 (s, 1H), 9.65 (s, 1H), 9.06 (s, 1H), 8.27 (dd, *J* = 17.6 Hz, 11.6 Hz, 1H), 6.63 (d, *J* = 18 Hz, 1H), 6.44 (d, *J* = 11.6 Hz, 1H), 6.18 (d, *J* = 19.6 Hz, 1H), 5.23 (m, 2H), 4.82 (m, 1H), 4.59 (q, *J* = 8.8 Hz, 2H), 4.08 (m, 4H), 3.73 (m, 4H), 3.61 (m, 4H), 3.54 (m, 4H), 3.50 (s, 3H), 3.49 (s, 3H), 3.48 (s, 3H), 3.42 (m, 4H), 3.41 (m, 4H), 3.29 (m, 4H), 3.24 (s, 3H), 3.19 (m, 4H), 3.11 (s, 3H), 3.06 (s, 3H), 3.04 (m, 4H), 2.66 (m, 1H), 2.27 (m, 2H), 2.15 (m, 2H), 1.67 (m, 3H), 1.65 (m, 3H), -1.64 (s, 1H), -1.66 (s, 1H). <sup>13</sup>C NMR (100.6 MHz, CDCl<sub>3</sub>)  $\delta$  173.5, 173.1, 172.5, 169.7, 168.8, 154.7, 148.8, 142.9, 139.4, 136.4, 135.9, 135.5, 135.3, 134.7, 130.5, 129.3, 127.8, 123.5, 121.7, 102.4, 102.1, 98.6, 93.5, 72.5, 71.9, 71.7, 70.7, 70.6, 70.5, 70.4, 70.3, 70.1, 70.0, 69.2, 68.9, 68.8, 66.8, 65.0, 64.3, 63.5, 61.7, 59.0, 58.9, 58.7, 53.0, 49.3, 41.5, 38.6, 31.0, 29.7, 23.8, 19.6, 17.6, 14.0, 12.4. HRMS (ESI) *m/z* calcd for [C<sub>55</sub>H<sub>78</sub>N<sub>4</sub>O<sub>15</sub> + Na]<sup>+</sup> 1057.535, found 1057.540. (ESI) *m/z* calcd for C<sub>55</sub>H<sub>79</sub>N<sub>4</sub>O<sub>15</sub> [M + H]<sup>+</sup> 1035.5536, found 1035.5538. UV-vis (CHCl<sub>3</sub>)  $\lambda_{\max}$  ( $\epsilon/M^{-1}cm^{-1}$ ) 665 nm (89000), 404 nm (309333).

**Hydrolytic Stability and Intrinsic Solubility.** For the hydrolytic stabilities, solutions of **1–3** were prepared in 9:1 methanol/water and were adjusted to pH = 2 or 8 with either formic acid or ammonium hydroxide. The samples were then injected in the LC-MS after 5 min, 1 h, and 4 h periods of time. The percent of starting **1–3** hydrolyzed was reported based on the reduction in LC-MS chromatogram peak area and total ion abundance. For the intrinsic solubilities, aliquots of 1% (v/v) DMSO/water were added to 50  $\mu$ g quantities of chlorin  $e_6$  or **1–3**, where the solutions were stirred for 1 h at room temperature and then allowed to stand for 5 h. The solution was filtered to separate insoluble compounds, and the amount of compound in the filtrate was determined by monitoring the Soret bands of chlorin  $e_6$  and **1–3**.

**Computations.** Octanol/water partition calculations were conducted with the ACD method.<sup>18</sup> Monte Carlo calculations were conducted with Hyperchem 8.0,<sup>20</sup> and graphical representations of the molecules were generated with ChemBio3D Ultra.<sup>41</sup> Conformations were searched by the Monte Carlo method with the MM+ force field in the gas phase. Approximately 200 conformations were optimized for **1**, ~100 conformations for **2**, and 27 conformations for **3**. For each chlorin **1–3**, the lowest 10 energy MM+ optimized conformations were then optimized with B3LYP/6-31G(d) in the gas phase, and the lowest energy B3LYP structure is shown in Figure 3. Vibrational analyses were carried out with Gaussview software.<sup>42</sup>

**Cell Culture Conditions.** Human ovarian carcinoma cells (OVCAR-5), purchased commercially, were grown and maintained in RPMI 1640 media supplemented with 10% fetal calf serum and 1% of 5,000 IU/mL penicillin/streptomycin, referred to as "complete media". The cell line was maintained at 37 °C in humidified 5% CO<sub>2</sub> atmosphere.

**Cellular Uptake.** The cellular uptake of the photosensitizers chlorin  $e_6$  and **1–3** in the total cell population was determined as described previously.<sup>4</sup> Twenty-four hours before the cellular uptake experiment, 85,000 OVCAR-5 cells were seeded in 24-well tissue culture plates in complete media and incubated at 37 °C to achieve ~80% confluency. Thereafter, fresh complete media containing the different concentrations (0.5–4.0  $\mu$ M) of the photosensitizer under test was added under subdued light conditions, and the samples were incubated for 4 h. After incubation, the cellular uptake was terminated by washing the cells 3 times with PBS. The cells were then dissolved in 800  $\mu$ L of 0.1 M NaOH/1% SDS and placed on a shaker at room

temperature for 24 h. The concentration of the photosensitizer was quantified by measuring the fluorescence ( $\lambda_{\text{ex}} = 400 \text{ nm}$ ,  $\lambda_{\text{em}} = 580\text{--}700 \text{ nm}$ ) using a microplate reader followed by calculation of the peak area. The concentration of photosensitizer was determined by comparison with calibration curves obtained with known concentration of each photosensitizer in 0.1 M NaOH/1% SDS and expressed as the number of moles. The protein content of the total cell population per well was then determined using a BCA protein assay kit, and the calibration curves were prepared from known concentrations of BSA prepared in 0.1 M NaOH/1% SDS. Results were expressed as moles of the photosensitizer per microgram of cell protein. All experiments were performed in triplicate and were repeated three independent times.

**Subcellular Localization of the Chlorin Photosensitizers.** The subcellular localization of the photosensitizers in OVCAR-5 cells was investigated by confocal microscopy using the Olympus confocal microscope. Briefly, 42,500 OVCAR-5 cells were seeded in a glass-bottom 24-well tissue culture plates in complete media and incubated at 37 °C allowed to adhere overnight. The cells were then incubated for 4 h with fresh complete media containing 1  $\mu\text{M}$  concentration of each photosensitizer and incubated in the dark at 37 °C. In the final 30 min, a mitochondrial, Mitotracker Green FM or a lysosomal, LysoTracker Green DND-26, green fluorophore was added into the media at a final concentration of 50 nM. At the end of 4 h of incubation, the cells were washed three times with warm PBS, followed by addition of 1 mL of cold PBS and observed under a laser-scanning confocal microscope. The fluorescent images were acquired with confocal software using a 20 $\times$  objective lens and zoomed in 5 $\times$ .

**Phototoxicity Studies.** Approximately 85,000 OVCAR-5 cells in complete media were seeded into each well of 24-well culture plates overnight to attain ~80% confluency. Fresh complete media containing (i) no photosensitizer (as the “no” treatment control) or (ii) 0.01, 0.1, or 1  $\mu\text{M}$  chlorin  $e_6$  or 1–3 were added in triplicate and incubated for 4 h at 37 °C. Thereafter, the cells were washed three times with PBS, fresh complete media was added, and the cells were irradiated with the 670 nm laser or not for dark controls (DT). A CW diode laser was used as described previously.<sup>43</sup> Briefly, 670-nm laser light was delivered through the bottom of each well on clear plastic via a vertically mounted multimode FT-600-EMT fiber optic connected to a 5-cm long cylindrical light diffuser, which was collimated to overfill the well area for nearly uniform light delivery. An energy power meter was used, and cells were irradiated with a 2, 5, or 10 J/cm<sup>2</sup> dose and an irradiance of 50 mW/cm<sup>2</sup>. After treatment, cells were further incubated for 24 h, and then MTT assay was used to measure the cell viability. The survival fraction was calculated compared to no treatment controls.

**Quenching Studies.** Approximately 85,000 OVCAR-5 cells in complete media were seeded into each well of 24-well plates, and the culture plates were incubated overnight at 37 °C to attain ~80% confluency. Fresh complete media containing (i) no photosensitizer (i.e., the “no” treatment control) or (ii) chlorin  $e_6$  or 1–3, in triplicate, was added into the respective wells and then incubated for 4 h at 37 °C with 30 mM mannitol or 2 mM sodium azide being added to the test wells 1 h prior to illumination. Thereafter, the cells were washed three times with PBS, then D<sub>2</sub>O-based media with or without 30 mM mannitol or 2 mM sodium azide was added to the respective wells, and the cells were irradiated with 670 nm laser with 5 J/cm<sup>2</sup> fluence at an irradiance of 50 mW/cm<sup>2</sup> [or not for dark controls (DT)]. After irradiation, D<sub>2</sub>O-based media was replaced with complete media, and the cells were further incubated for 24 h followed by analysis of the cell viability using MTT assay. The survival fraction was calculated compared to no treatment controls.

**Lifetime Measurements.** The singlet oxygen lifetime was determined using a 10-Hz Nd:YAG Q-switched laser producing 355 nm and ~2 mJ/pulse and a photomultiplier tube at an operating voltage of –650 V. Five milliliter solutions were used containing 2 (5.2  $\times 10^{-5}$  M). The <sup>1</sup>O<sub>2</sub> luminescence intensity was monitored through a NIR bandpass filter centered at 1270 nm (OD4 blocking, fwhm = 15 nm). The <sup>1</sup>O<sub>2</sub> luminescence signals were registered on a 600 MHz

oscilloscope, and the kinetic data for the lifetime were determined by a least-squares curve-fitting procedure.

## ■ ASSOCIATED CONTENT

### 📄 Supporting Information

Spectroscopic data for compounds 1–3. This material is available free of charge via the Internet at <http://pubs.acs.org>.

## ■ AUTHOR INFORMATION

### Corresponding Author

\*E-mail: [thasan@partners.org](mailto:thasan@partners.org); [agreer@brooklyn.cuny.edu](mailto:agreer@brooklyn.cuny.edu)

### Notes

The authors declare no competing financial interest.

## ■ ACKNOWLEDGMENTS

S.K., G.G., A.G., B.R., D.B., and A.G. acknowledge support from the NIH-National Institute of General Medical Sciences (SC1GM093830). Grant support to T.H. was provided by the NIH-National Cancer Institute (5R01CA160998). B.R. is the recipient of a Barry M. Goldwater Scholarship and the Arnold and Ruth T. Kaufman Undergraduate Chemistry Research Award at Brooklyn College. Computational support was provided by the College of Staten Island CUNY High Performance Computing Facility. We also thank Leda Lee for the graphic arts work.

## ■ REFERENCES

- (1) Roberts, W. G.; Shiau, F.-Y.; Nelson, J. S.; Smith, K. M.; Berns, M. W. *J. Nat. Cancer Inst.* **1988**, *80*, 330–336.
- (2) Hamblin, M. R.; Miller, J. L.; Rizvi, I.; Ortel, B.; Maytin, E. V.; Hasan, T. *Cancer Res.* **2001**, *61*, 7155–7162.
- (3) O’Shea, D. F.; Miller, M. A.; Matsueda, H.; Lindsey, J. S. *Inorg. Chem.* **1996**, *35*, 7325–7338.
- (4) Hamblin, M. R.; Miller, J. L.; Ortel, B. *Photochem. Photobiol.* **2000**, *72*, 533–540.
- (5) Tijerina, M.; Kopečková, P.; Kopeček, J. *J. Controlled Release* **2001**, *74*, 269–273.
- (6) Kozyrev, A. N.; Chen, Y.; Goswami, L. N.; Tabaczynski, W. A.; Pandey, R. K. *J. Org. Chem.* **2006**, *71*, 1949–1960.
- (7) Hargus, J. A.; Fronczek, F. R.; Graca, M.; Vicente, H.; Smith, K. M. *Photochem. Photobiol.* **2007**, *83*, 1006–1015.
- (8) Aksenova, A. A.; L., Sebyakin, Yu. L.; Mironov, A. F. *Russ. J. Bioorg. Chem.* **2001**, *27*, 124–129.
- (9) Kim, H.-K.; Van den Bossche, J.; Hyun, S.-H.; Thompson, D. H. *Bioconjugate Chem.* **2012**, *23*, 2071–2077.
- (10) Xu, H.; Deng, Y.; Chen, D.; Hong, W.; Lu, Y.; Dong, X. *J. Controlled Release* **2008**, *130*, 238–245.
- (11) Nakamura, H.; Fang, J.; Gahininath, B.; Tsukigawa, K.; Maeda, H. *J. Controlled Release* **2011**, *155*, 367–375.
- (12) Zalipsky, S.; Lee, C. Use of functionalized polyethylene glycols for modification of polypeptides. In *Poly(ethylene glycol) Chemistry. Biotechnological and Biomedical Applications*; Harris, M. J., Ed.; Plenum Press, New York, 1992; pp 347–370.
- (13) Lavis, L. D. *ACS Chem. Biol.* **2008**, *3*, 203–206.
- (14) Fleming, A. B.; Haverstick, K.; Saltzman, W. M. *Bioconjugate Chem.* **2004**, *15*, 1364–1375.
- (15) Marcus, Y.; Sasson, K.; Fridkin, M.; Shechter, Y. *J. Med. Chem.* **2008**, *51*, 4300–4305.
- (16) Tetko, I. V.; Poda, G. I. *J. Med. Chem.* **2004**, *47*, 5601–5604.
- (17) McGill, N. W.; Williams, S. J. *J. Org. Chem.* **2009**, *74*, 9388–9398.
- (18) Zhu, J.; Deur, C.; Hegedus, L. S. *J. Org. Chem.* **1997**, *62*, 7704–7710.
- (19) *ACD Program*; Advanced Chemistry Development Inc.: Toronto, ON, Canada.

- (19) Hirohara, S.; Obata, M.; Ogata, S. I.; Kajiwaru, K.; Ohtsuki, C.; Tanihara, M.; Yano, S. *J. Photochem Photobiol. B: Biol.* **2006**, *84*, 56–63.
- (20) *Hyperchem 8.0*; Hypercube, Inc.: Gainesville, FL.
- (21) Frisch, M. J.; Trucks, G. W.; Schlegel, H. B.; Scuseria, G. E.; Robb, M. A.; Cheeseman, J. R.; Scalmani, G.; Barone, V.; Mennucci, B.; Petersson, G. A.; Nakatsuji, H.; Caricato, M.; Li, X.; Hratchian, H. P.; Izmaylov, A. F.; Bloino, J.; Zheng, G.; Sonnenberg, J. L.; Hada, M.; Ehara, M.; Toyota, K.; Fukuda, R.; Hasegawa, J.; Ishida, M.; Nakajima, T.; Honda, Y.; Kitao, O.; Nakai, H.; Vreven, T.; Montgomery, J. A., Jr.; Peralta, J. E.; Ogliaro, F.; Bearpark, M.; Heyd, J. J.; Brothers, E.; Kudin, K. N.; Staroverov, V. N.; Kobayashi, R.; Normand, J.; Raghavachari, K.; Rendell, A.; Burant, J. C.; Iyengar, S. S.; Tomasi, J.; Cossi, M.; Rega, N.; Millam, N. J.; Klene, M.; Knox, J. E.; Cross, J. B.; Bakken, V.; Adamo, C.; Jaramillo, J.; Gomperts, R.; Stratmann, R. E.; Yazyev, O.; Austin, A. J.; Cammi, R.; Pomelli, C.; Ochterski, J. W.; Martin, R. L.; Morokuma, K.; Zakrzewski, V. G.; Voth, G. A.; Salvador, P.; Dannenberg, J. J.; Dapprich, S.; Daniels, A. D.; Farkas, O.; Foresman, J. B.; Ortiz, J. V.; Cioslowski, J.; Fox, D. J. *Gaussian 09, Revision A.1*; Gaussian Inc.: Wallingford, CT, 2009.
- (22) Li, Y.-C.; Rissanen, S.; Stepniewski, M.; Cramariuc, O.; Róg, T.; Mirza, S.; Xhaard, H.; Wytrwal, M.; Kepczynski, M.; Bunker, A. *J. Phys. Chem. B* **2012**, *116*, 7334–7341.
- (23) Chefurka, W.; Chatelier, R. C.; Sawyer, W. H. *Biochim. Biophys. Acta* **1987**, *896*, 181–186.
- (24) Arun, K. T.; Epe, B.; Ramaiah, D. *J. Phys. Chem. B* **2002**, *106*, 11622–11627.
- (25) Dsouza, R. N.; Pischel, U.; Nau, W. M. *Chem. Rev.* **2011**, *111*, 7941–7980.
- (26) Laville, I.; Figueiredo, T.; Loock, B.; Pigaglio, S.; Maillard, P.; Grierson, D. S.; Carrez, D.; Croisy, A.; Blais, A. *Bioorg. Med. Chem.* **2003**, *11*, 1643–1652.
- (27) Roberts, W. G.; Berns, M. W. *Lasers Surg. Med.* **1989**, *9*, 90–101.
- (28) Mojzisoava, H.; Bonneau, S.; Vever-Bizet, C.; Brault, D. *Biochim. Biophys. Acta, Biomembr.* **2007**, *1768*, 2748–2756.
- (29) Ogilby, P. R.; Foote, C. S. *J. Am. Chem. Soc.* **1982**, *104*, 2069–2070.
- (30) Rancan, F.; Maeda, H.; Böhm, F.; Röder, B. *Bioconjugate Chem.* **2007**, *18*, 494–499.
- (31) Jensen, R. L.; Arnbjerg, J.; Ogilby, P. R. *J. Am. Chem. Soc.* **2010**, *132*, 8098–8105.
- (32) Skovsen, E.; Snyder, J. W.; Lambert, J. D. C.; Ogilby, P. R. *J. Phys. Chem. B* **2005**, *109*, 8570–8573.
- (33) Jensen, R. L.; Arnbjerg, J.; Ogilby, P. R. *J. Am. Chem. Soc.* **2012**, *134*, 9820–9826.
- (34) Redmond, R. W.; Kochevar, I. E. *Photochem. Photobiol.* **2006**, *82*, 1178–1186.
- (35) Engst, P.; Kubat, P.; Jirsa, M. *J. Photochem. Photobiol. A: Chem.* **1994**, *78*, 215–219.
- (36) Rodgers, M. A. J.; Snowden, P. T. *J. Am. Chem. Soc.* **1982**, *104*, 5541–5543.
- (37) Davidson, R. S.; Trethewey, K. R. *J. Am. Chem. Soc.* **1976**, *98*, 4008–4009.
- (38) Huang, L.; St. Denis, T. G.; Xuan, Y.; Huang, Y. Y.; Tanaka, M.; Zadio, A.; Sarna, T.; Hamblin, M. R. *Free Radic. Biol. Med.* **2012**, DOI: 10.1016/j.freeradbiomed.2012.09.006.
- (39) Bartusik, D.; Aebischer, D.; Ghosh, G.; Minnis, M.; Greer, A. *J. Org. Chem.* **2012**, *77*, 4557–4565.
- (40) Mahendran, A.; Vuong, A.; Aebischer, D.; Gong, Y.; Bittman, R.; Arthur, G.; Kawamura, A.; Greer, A. *J. Org. Chem.* **2010**, *75*, 5549–5557.
- (41) *ChemBio3D Ultra 12.0*; CambridgeSoft Corporation: Cambridge, U.K.
- (42) Dennington, R.; Keith, T.; Millam, J. *GaussView, Version 5*; Semichem Inc.: Shawnee Mission, KS, 2009.
- (43) Celli, J. P.; Solban, N.; Liang, A.; Pereira, S. P.; Hasan, T. *Lasers Surg. Med.* **2011**, *43*, 565–574.